MSUCL-232
December 1976

Levels of ^{52}Fe Studied with the (p,t) Reaction*

P. Decowski,** W. Benenson, B.A. Brown, and H. Nann

Cyclotron Laboratory and Physics Department
Michigan State University, East Lansing, Michigan 48824

Abstract: The ^{54}Fe(p,t)^{52}Fe reaction at 45 MeV has been used to study states of ^{52}Fe. Characteristic L-transfers in the angular distributions were used to assign ~60 spins and parities. An $f_{7/2}$ shell model, with admixtures calculated in first order perturbation theory, successfully accounts for both the location and strength of many of the observed levels.

NUCLEAR REACTIONS ^{54}Fe(p,t) E = 45 MeV. E_x = 0 - 10.33 MeV measured angular distributions. Enriched target. Magnetic spectrograph. Shell model calculation.

---

*Work supported in part by the National Science Foundation.

**On leave from the Institute of Experimental Physics of the University of Warsaw.

1. Introduction

Studies of the ^{52}Fe nucleus are important for understanding nuclear structure in the upper part of the $f_{7/2}$ shell. The structure of this nucleus has been investigated in the past with the (^{3}He,n)[1,2] and (p,t) reactions[3-6]. Spins and parities were assigned only to the most strongly excited states, which are characterized mainly by L=0,2, and 4 angular momentum transfers. Many of the weaker states remained unassigned, and there existed several controversies concerning even the stronger states.

The present high resolution experiment permit the finding of spins and parities for about 60 levels with excitation energies up to 10 MeV. The comparison of the measured cross sections with the DWBA calculations provide some information about the distribution of $f_{7/2}^{-2}$ strength among the states. Admixtures of other orbitals which would drastically affect the cross section especially for L=0 are accounted for by a first order perturbation theory calculation.

2. Experiment

A beam of protons accelerated to an energy of 45 MeV by the Michigan State University Cyclotron bombarded a 250 μg/cm^2 target of ^{54}Fe enriched to 96.7%, which was deposited on 20 μg/cm^2 ^{12}C foil. The position of triton groups on the focal plane of an Enge split-pole spectrograph was measured by a delay-line counter[7] backed with proportional and scintillation counters which provided energy loss and time-of-flight

measurements for discrimination against other particles. The average resolution (FWHM) was ≈15 keV. The length of the position sensitive counter (25 cm) corresponded to ≈5 MeV interval in excitation energy.

The angular distributions were measured in the 6°-60° angular range in 2° steps at forward angles, and 3°-5° steps at more backward angles. For each angle the target was exposed to the beam for a total charge of 1-10 mC.

3. Results

The spectrum of tritons measured at 14° is shown in fig. 1 The only impurities present come from carbon, oxygen, and the 2.3% admixture of ^{56}Fe in the target. The intensities of the peaks were extracted from measured spectra by a fitting procedure which used experimental line shapes derived from the most intense peaks. The cross sections were obtained by normalizing measured yield to the yield of protons elastically scattered from the same target. The elastic scattering cross section was calculated with typical proton optical model parameters[8]). The resulting target thickness agreed with α-particle energy loss measurements to within 15%.

The measured angular distributions are shown in fig. 2 and 3. They exhibit features prominent enough to make a distinction between different L-transfers for all the stronger states. One step two-neutron pickup excites only natural parity states (assuming the transfered neutron pair is in a S=0 configuration), and since the target is 0^+ it was possible to infer spins and parities of the observed states from the L-transfer. They are

listed together with excitation energies in Table 1.

The measured excitation energies are free from the error connected with the nonlinearities of the delay-line counter. This was achieved by calibrating the counter using the positions of the triton group corresponding to the ground state of ^{10}C at many different settings of the spectrograph magnetic field. The isospin assignments in Table I are based on the correspondence to the parent nuclei, ^{52}Mn for T=1 and ^{52}Cr for T=2. For ^{52}Mn this included a comparison to the L-transfer observed in the ^{54}Fe (p,^{3}He) reaction[9]).

3.1. L=0 TRANSITIONS

The prominent oscillatory character of the angular distributions for these transitions allows one to distinguish them unambiguously from other transitions. Ten transitions were identified as L=0 in the excitation region investigated. The strongest ones lead to the ground state and to the 0^+, T=2 state found in earlier works near 8.5 MeV.[1-4,6]) The present experiment shows that in fact the 0^+,T=2 state is split into two states separated by about 4 keV but the energy resolution was not good enough to measure both angular distributions separately. Such splitting is a common occurence for nuclei in the $f_{7/2}$ shell.[10])

3.2 L=2 TRANSITIONS

The characteristic feature of the experimental L=2 transitions is the occurrence of minima at 25°-27° and 47°. There are two types of shapes which differ at forward angles. They

are grouped in fig. 2. The strongest transitions excite the first 2^+, T=0 state and first 2^+, T=1 state, which again appears to be split into two states 10±1 keV apart. In ref. [3]), an assignment $J^\pi=4^+$ was made for a state at 6.02 MeV as well as for a state at 8.33 MeV and is therefore in contradiction with the present work.

Direct measurement of the angular distribution of 2.762 MeV state was not possible because it was obscured by tritons from the 6.325 MeV, 3^- state which is strongly excited in the (p,t) reaction on the ^{56}Fe admixture in the target. The extraction of this contribution is based on the measured cross section for the ^{56}Fe(p,t)^{54}Fe reaction at the same energy[11]) and yielded an L=2 angular distribution in agreement with the 2^+ assignment for this state in ref. [1]).

3.3 L=4 TRANSITIONS

The angular distributions for L=4 and L=3 transitions often are quite similar, and it is necessary to be very careful in the identification. The following experimental criteria were used: L=4 angular distributions have a maximum at 15°-17° (though not always well pronounced) and a minimum at 37°-40°, whereas L=3 angular distributions are peaked forward and have minima at 32°-35° and 55°-57°. The strongest L=4 transition is to the 4^+, (T=1) state at 6.416 MeV. Ref. [3]) identified this state as 5^-. The difference between experimental angular distributions for L=4 and L=5 transitions measured in the present experiment is large enough to rule out this possibility. Our

assignments of spin and parity 4^+ for the states at 3.583 MeV and 6.714 MeV do not agree with the 2^+ assignments of ref. [3]), but in the case of 3.583 MeV level it does agree with the result of ref. [1]).

3.4 L=6 TRANSITIONS

The main feature of these transitions is peaking around 30°. Essentially there are two kinds of experimental shapes grouped in fig. 3: one type with a relatively deep minimum around 15°, and another with a much broader distribution. In contrast to distributions for known 6^+ states at 5.65 and 4.33 MeV some distributions do not rise at forward angles which makes L=6 assignment for them questionable. The strongest transitions lead to the analog of the ^{52}Mn, 6^+,T=1 ground state at 5.652 MeV and to the 6^+ (T=1) state at 7.611 MeV. The angular distribution of the strong transition to the state at 8.962 MeV has a shape which suggests admixture of another L-value (probably 4 or 5) from an unresolved nearby state. The present assignment of spin and parity (6^+) to the state at 4.869 MeV does not agree with the tentative assignment of 5^- in ref. [3]).

3.5 ODD L TRANSITIONS

One of the most strongly excited states is at 4.400 MeV with an L=3 angular distribution. In previous (p,t) work[3]) this state was identified as 4^+. The strong excitation of this state and its low energy suggest that it is the collective octupole vibration which occurs in all f-p shell nuclei around this energy. One 5^- state observed at 5.134 MeV (in ref. [3]) it was tentative

identified as 3^- .

4. DWBA analysis and discussion

Up to the present, a theory which can account for all states observed in ^{52}Fe has not been attempted. However, calculations assuming $1f_{7/2}^{-4}$ configurations which account for many of the positive parity levels have been carried out[14]). Since the excitation energies and electromagnetic transition strengths for many of the levels in ^{54}Fe and ^{52}Fe seem to be well described by the $f_{7/2}^{n}$ wave functions[15-16]), DWBA calculations were performed with the zero-range code DWUCK under the assumption of pure $f_{7/2}$ two-neutron pickup. As will be discussed below, the pickup strength is strongly enhanced by the coherent contributions of many orbitals, especially for L=0. However, the dominant effect of these contributions can be treated as an overall enhancement factor since the amplitudes for configurations outside the $f_{7/2}$ shell are small (and hence perturbation theory can be applied) and since the DWBA angular distributions are insensitive to the particular orbits involved in the two-neutron pickup.

The optical model parameters listed in Table 2 were the same as used in ref. [12]). Examples of DWBA fits with pure $f_{7/2}^{2}$ pickup for positive parity states are shown in fig. 4. The shapes of these calculated angular distributions depend very little on the details of the radial form factors. They are mainly determined by the distorted waves in the entrance and exit channels. Because of the rather large mismatch in angular momentum, zero-range DWBA calculations are not able to produce good fits to the shapes of the experimental L=6 angular distributions.

This leads to a problem in evaluating the 6^+ strengths, as will be discussed below.

The experimental cross sections were compared with DWUCK cross sections using the formula:

$$\sigma_{exp} = 9.72(\varepsilon D_o^2)(S^{1/2})^2(2J+1)^{-1}\sigma_{DWUCK}$$

σ_{exp} and σ_{DWUCK} are the experimental and DWBA cross sections integrated over the angular interval 6°-60°. The constant 9.72 accounts for the details of the triton wave function and the range of the interaction[13]), whereas εD_o^2 is a normalization factor which will be discussed later. The spectroscopic amplitude, $S_{1/2}$, in the case of pickup of two neutrons coupled to spin J from a filled shell, is $(2J+1)^{1/2}a$. The quantity a^2 is the probability of the $(f_{7/2}^{-2})_J$ neutron configuration in the final state.

Thus, for each level a multiplicative factor $\varepsilon D_o^2 a^2$ was extracted from the DWBA analysis. The relative values of a^2 were compared with the predictions of a $f_{7/2}^{n}$ shell-model calculation by normalizing εD_o^2 to the state which should carry the most pure $f_{7/2}^{-2}$ strength for each L-transfer. These were isolated, strongly excited states which correspond closely in excitation energy to calculated energies. The following states were chosen: 0^+,T=2 8.56 MeV; 2^+, T=2 10.01 MeV; 4^+ - the sum of the strengths of the two lowest T=1 states at 6.42 MeV and 8.54 MeV (compared with the sum of the strengths for the lowest T=1 theoretical states); 6^+ - lowest T=1 state at 5.56 MeV. The experimental normalization factors εD_o^2 obtained this way for each spin are listed in the second column of Table 3. The

extracted pickup strengths are compared with the theoretical $f_{7/2}$ strengths a^2 in Tables 4-7 and in fig. 5.

The $f_{7/2}^{n}$ calculations were carried out with the eight two-body matrix elements with J=0-7 taken from the experimentally observed ^{54}Co energy levels which are thought to have predominantly $f_{7/2}^{-2}$ configurations[14]). These levels are 0, 937, 1446, 2278, 2630, 2151, 3085, and 199 keV for J=0 through 7, respectively. With these matrix elements the $T_{1/2}$=56 sec, isomeric 12^+ level in ^{52}Fe (ref. [15])) is predicted at 6.974 MeV compared with the observed energy of 6.83±0.25 MeV. It also predicts correctly that the 10^+ state lies above the 12^+ state. The wave functions for ^{52}Fe were obtained in the proton-neutron coupling scheme in the form

$$|J_\alpha> = \sum_{J_p J_n} a(J_p,J_n,J_\alpha)|j_p^{-2}(J_p)\ j_n^{-2}\ (J_n)\ J_\alpha>$$

where α distinguishes states with the same J. The ^{54}Fe wave function is $|j_p^{-2}(J_p=0)>$ is this model. The (p,t) amplitudes are then just $[a(J_p=0,J_n=J_\alpha=L,J_\alpha)]$.

The experimental and theoretical pickup strengths summed over all the 0^+ states given in Table 4 are in good agreement. The strength of the theoretical state at 7.53 MeV appears to be divided among seven additional states. This large number of 0^+ states can be accounted for by excited seniority-zero states as well as states originating from the seniority-four couplings of excited states in ^{54}Fe below 4 MeV. The importance of using an exact $f_{7/2}$ shell-model as opposed to the simple pairing model[17]) or pure seniority $f_{7/2}$ model[13]) is shown by the ratio of the cross sections for the T=0 ground-state to the T=2,

8.56 MeV state. The latter models assume that the ^{52}Fe ground and $T=2,0^+$ state have pure seniority-zero, in which case their cross section ratio is given by isospin Clebsch-Gordan coefficients to be 3. In the exact $f_{7/2}$ calculation this ratio is 2.23 as compared with the experimental value of 2.04.

The general features of the comparison with the $f_{7/2}$ theory for $J=0^+-6^+$ is that the relative cross sections are best described in the case of isolated experimental and theoretical levels, but also that many other levels are observed the summed strength of which corresponds approximately to the predicted strength for a single state. This is just the situation which would be expected if the ground state of ^{54}Fe were predominantly $f_{7/2}^{-2}$ and the excited states in ^{52}Fe were $f_{7/2}^{-4}$ mixed with core excited configurations. It is interesting to note however that the yrast levels in ^{52}Fe are less and less well described by a single $f_{7/2}$ state as they go from $J=0^+$ to $J=6^+$; for example, the $f_{7/2}$ strength for the 6^+ state predicted at 4.33 MeV is found experimentally mostly in the two states at 4.33 and 4.87 MeV. Presumably this situation reverses as one goes from $J=8^+$ to $J=12^+$ since there are few shell-model configurations which can form $J=12^+$.

The distribution of pickup strength is well reproduced in the $f_{7/2}$ model except for enhanced L=2 strength for the ten 2^+ states from 2.76 to 9.04 MeV. This L=2 enhancement may be due to 1p-3h admixtures in the ^{54}Fe ground state or may be an indication of some two-step contributions to the reaction mechanism. In addition both the L=0 and 2 strengths for some states which do not have $f_{7/2}^{-4}$ configuration may be due to the direct pickup of two $1d_{3/2}$ neutrons. However the weakness of those states might

be accounted for by including mixing with other states.

The normalization factors εD_o^2 given in Table 3 show a large variation with J. The large value of εD_o^2 for J=0 indicates the enhanced probability of finding two neutrons in a relative 0s-state at the nuclear surface. This enhancement can be found in the shell model when a large number of orbitals, at least all the orbitals in a major shell, are coherently mixed via a short range attractive interaction. In its extreme this coherence leads to the BCS pairing model, a model which appears to work best, for example, in the Pb isotopes where most of the J=0 sum rule limit is found in ground states[18]).

In the $f_{7/2}$ shell the $f_{7/2}^n$ component dominates the wave function and therefore the effect of the two-nucleon correlations can be estimated in perturbation theory. The situation for $^{54}Fe(p,t)^{52}Fe$ reaction is illustrated diagrammatically in fig. 6. Fig. 6a shows the zeroth order process, which is the result of the two neutron annihilation operator[19]) $M_J=-\sum_{j_n}(j_n+1/2)^{1/2}A[(j_n^2)_J]$ acting on the initial state of two proton holes with $J_p=0$ and a filled shell of neutrons. Figure 6b represents the effect of the admixture of two neutron holes in the 1d-2s orbitals in the final state, and fig. 6c represents the admixture of two neutron particles in the $2p\text{-}1f_{5/2}\text{-}1g_{9/2}$ orbitals in the initial state. The zeroth order process gives $S^{1/2}(2J+1)^{-1/2}=1$, and the amplitudes for the first order processes (figs. 6b and c) are

$$\frac{S^{1/2}(j_n'j_n'')}{(2J+1)^{1/2}} = \frac{-\langle j_n^2\ J|V|j_n'j_n''\ J\rangle}{|\varepsilon(j_n') + \varepsilon(j_n'')-2\varepsilon(j_n)|} \qquad (1)$$

These have been calculated with a delta function two-body interaction adjusted to give the $f_{7/2}^2$,J=0-6 splitting of 3.085 MeV and with the single particle energies appropriate for ^{56}Ni taken from Harvey and Khanna[20]). The results are given in Table 8.

The enhancement factor ε was then calculated from the expression

$$\varepsilon = [1+ \sum_{j_n',j_n''\neq j_n} \delta(j_n'j_n'')]^2$$

where

$$\delta(j_n'j_n'') = \frac{S^{1/2}(j_n'j_n'')\left[\sigma^{max}_{DWUCK}(j_n'j_n'')\right]^{1/2}}{(2J+1)^{1/2}\left[\sigma^{max}_{DWUCK}(j_n^2=f_{7/2}^2)\right]^{1/2}} \qquad (2)$$

The ratio of the square root of the DWUCK cross sections, includir the appropraite phase factor, was obtained at an angle for a maximum in the angular distribution for each J; ~ 20°, ~ 32°, ~17° and ~ 38° for J=0-6, respectively. This is justified because the ratios of the DWBA angular distributions are nearly independer of angle. In addition the ratios of the DWUCK cross sections are not very sensitive to the Q-value over the range of excitation energies studied (see fig. 1 in ref. [21])). The values of $\delta(j_n'j_n'')$ are given in Table 8, and the enhancement factor ε is given in Table 3.

From fig. 6 one can see that the effect of the first order diagrams 6b and 6c is simply to renormalize the two-neutron trans operator by a factor ε which is independent of the detailed $f_{7/2}^n$ configurations involved. That is, except for the small Q-value dependence in δ and the single-particle energy dependence in eq. 1, the <u>same</u> value of ε should describe all two-neutron transfer processes in the $f_{7/2}$ shell. This renormalization effec

has been found experimentally for the (t,p) reactions on the Ca isotopes.[22])

Even though the probabilities of the core excited components are quite small, (16.6% and 1.5% for J=0 and 2, respectively) ϵ is very large especially for L=0 because the contributions are all coherent, and many of the configurations for example $(2s_{1/2})^2$ and $(2p_{3/2})^2$ have a large component of 0s relative motion. The monopole pairing is predominent, but there is also a large quadrupole pairing enhancement.

There are several first order and many higher order diagrams which cannot be considered as a renormalization of the $f_{7/2}{}^n$ amplitudes, but their effects are probably much less important than the ones discussed above. An example is fig. 6d which shows particles which are picked up from the $1f_{7/2}$ and $2p_{3/2}$ orbitals leaving ^{52}Fe in a state with the two protons in a 2^+ or 4^+ configuration. This diagram represents the (p,t) reaction amplitude due to the ^{54}Fe, $f_{7/2}{}^{-2}$ 2^+ or 4^+ states and thus obviously cannot be considered as enhancement factor. The size of this effect together with the dynamic effect of exciting these states in ^{54}Fe by a two step reaction process can be estimated experimentally from the enhancement of the J=2 cross section in ^{52}Fe as about 20-30% so of the total cross section. The contribution of these processess for the strongly excited, isolated $f_{7/2}{}^n$ states which were used to extract ϵD_o^2 is then probably $\leq$20%.

The experimental and theoretical enhancement factors are compared in Table 3. It is interesting to investigate the enhancement factor due to a major shell alone. Considering only the f-p configurations in Table 8, the enhancement factors are 2.40,

1.50, 1.10 and 1.00 for J=0-6, respectively. These values lead to an average D_o^2 of about 33 for J=0-4, which is a typical value needed in the sd shell using complete $(sd)^n$ wave functions[12]). An analysis[21]) of the (t,p) reaction for L=0 transfers over the entire periodic table using complete major shell wave functions yielded a similar average D_o^2 value (~32). For J=0 the enhancement factor would be 7.86 for the sum-rule[21]) $[\sigma = \sum_{j'} \sigma(j'^2)]$ which means that only about 30% of the fp shell sum-rule is exhausted in the ^{54}Fe ground state.

Finally the enhancement factors were calculated with all of the sd-fp-$g_{9/2}$ components given in Table 8, and an average value of D_o^2=20 was obtained for J=0-6. This still large value of D_o^2 can originate from the approximations made in the zero range DWBA calculation as well as from the neglections of additional pair correlation effects from orbitals further from the Fermi surface.[23]) An important phenomenological question is how many orbits need to be considered so that D_o^2 is independent of L. From Table 3 it appears that a major shell is probably not sufficient in this case since much of the J=0 and 2 enhancement comes from the sd shell.

In this mass region the L=6 pickup is the least affected of the L-values by configuration mixing. However, it is difficult to extract a believable enhancement factor in this case because the L=6 angular distributions are badly fitted by the zero-range DWBA. The large mismatch in ℓ-space enhances the cross section at larger angles. Because of the simple shell model structure for the L=6 pickup especially for the two lowest T=1 states it would be very instructive to carry out finite range DWBA

calculations to attempt to explain the angular distributions and the enhancement factor for these states.

5. Conclusions

The lack of wave functions for the ^{54}Fe and ^{52}Fe nuclei calculated in a full f-p shell model space does not allow a detailed comparison between theory and experiment. However, the $f_{7/2}$ shell calculations presented do describe reasonably well the strongest positive parity states, especially for the states with low spin. The (2p-2h) admixtures to the $f_{7/2}$ wave functions calculated in perturbation theory explain successfully the strong enhancement of L=0 transitions as well as the smaller enhancement of the L=2 and 4 transitions. Zero-range DWBA calculations do not reproduce in a satisfactory way the L=6 transitions and cannot account for the variety of angular distribution shapes.

One of the authors (P.D.) would like to express his appreciation for hospitality of the Cyclotron Laboratory staff during his stay at Michigan State University.

REFERENCES

1) W. Bohne, H. Fuchs, K. Grabisch, D. Hilscher, U. Jahnke, H. Kluge, T.G. Masterson, H. Morgenstern, Nucl. Phys. A245(1975)107.

2) D. Evers, W. Assmann, K. Rudolph, S.J. Skorka, Nucl. Phys. A198(1972)268.

3) J.B. Viano, Y. Dupont, J. Menet, Phys. Lett. 34B(1971)397.

4) T. Suehiro, Y. Ishizaki, H. Ogata, J. Kokane, Y. Saji, A. Stricker, Y. Sugiama, I. Nonaka, Phys. Lett 33B(1970) 468.

5) G. Bassani, N.M. Hintz, C.D. Kavaloski, Phys. Rev. 136 (1964)B1006.

6) G.T. Garvey, J. Cerny, R.H. Pehl, Phys. Rev. Lett. 12 (1964)726.

7) R.G. Markham, R.G.H. Robertson, Nucl. Instr. and Meth. 129(1975)131.

8) F.D. Becchetti, G.W. Greenlees, Phys. Rev. 182(1968)1190.

9) A. Guichard, W. Benenson, H. Nann, Phys. Rev. C11(1975)2027.

10) A. Moalem, M.A.M. Shahabuddin, R.G. Markham, H. Nann, Phys. Lett. 58B(1975)286.

11) A. Saha, H. Nann (unpublished).

12) H. Nann, B.H. Wildenthal, Phys. Rev. C13(1976)1009.

13) H.W. Baer, J.J. Kraushaar, C.E. Moss, N.S.P. King, R.E.L. Green, P.D. Kuntz, E. Rost, Annals of Physics 76(1973)437.

14) W. Kutschera, B.A. Brown, K. Ogawa, submitted to Rivista del Nuovo Cimento.

15) D.F. Geesaman, R. Malmin, R.L. McGrath, J.W. Noé and J. Cerny, Phys. Rev. Letters 34(1975)326.

16) B.A. Brown, D.B. Fossan, J.M. McDonald and K.A. Snover, Phys. Rev. C9(1974)1033.

17) R.F. Casten, E.R. Flynn, Ole Hansen and J.T. Mulligan, Phys. Rev. C4(1974)130; B.F. Bayman and C.F. Clement, Phys. Rev. Letters 29(1969)1020.

18) S.M. Smith, P.G. Roos, A.M. Bernstein and C. Moazed, Nucl. Phys. A158(1970)497.

19) A. Bohr and B.R. Mottelson, Nuclear Structure, Vol. II, p. 641 (W.A. Benjamin, Inc., Reading Massachusetts, 1975).

20) M. Harvey and F.C. Khanna, Nucl. Phys. A221(1974)77.

21) R.A. Broglia, C. Riedel and T. Udagawa, Nucl. Phys. A184 (1973)23.

22) E.R. Flynn and O. Hansen, Phys. Letters 31B(1970)135.

23) R.A. Broglia, K. Kolltveit and B. Nilsson, Phys. Lett. 37B(1971)441.

Table 1--Excitation energies and spin-parity assignments for levels of ^{52}Fe

$(p,t)^{a)}$ E_p=45 MeV				$(p,t)^{b)}$ E_p=40 MeV		$(^3He,n)^{c)}$ $E_{^3He}$=13 MeV	
E_x(keV)	J^π		$\frac{\sigma_{int}}{2\pi}$(μb)	E_x(MeV)	J^π	E_x(MeV)	J^π
0	0^+		13.4	0.0	0^+	0.0	0^+
850 ± 5	2^+		6.0	0.84	2^+	0.84	2^+
2385 ± 5	4^+		1.5	2.36	4^+	2.36	4^+
2762 ± 5	2^+		0.27	2.74		2.75	2^+
3583 ± 5	4^+		1.3	3.55	2^+	3.59	4^+
4142 ± 10	0^+		0.57	4.14	0^+	4.16	0^+
4326 ± 8	6^+		0.55				
4400 ± 5	3^-		6.7	4.36	4^+		
4456 ± 8	2^+		0.44			4.43	2^+
4869 ± 15	(6^+)		0.44	4.86	(5^-)		
4896 ± 15			0.11				
5134 ± 8	5^-		2.7	5.11	(3^-)		
5328 ± 8	4^+		0.92				
5363 ± 5	0^+		3.1	5.31	0^+	5.36	0^+
5439 ± 15	(6^+)		0.32				
5483 ± 20	4^+		0.11				
5529 ± 20	4^+		0.10				
5563 ± 8	3^-		0.25				
5652 ± 8	6^+	T=1	1.6	5.65	6^+		
5718 ± 8	0^+		0.66			5.76	0^+
5792 ± 10			0.48	5.79			
5829 ± 5	2^+		0.88			5.82	2^+
5965 ± 15	4^+		0.26				

Table 1--Continued.

$(p,t)^{a)}$ E_p=45 MeV				$(p,t)^{b)}$ E_p=40 MeV		$(^3He,n)^{c)}$ $E_{^3He}$=13 MeV	
E_x(keV)	J^π		$\frac{\sigma_{int}}{2\pi}$(μb)	E_x(MeV)	J^π	E_x(MeV)	J^π
6034 ± 5	2^+	T=1	3.9	6.02	4^+	6.07	(2^+)
6044 ± 5	2^+		2.6				
6174 ± 15	6^+		0.23				
6231 ± 15			0.15				
6416 ± 5	4^+	(T=1)	4.7	6.38	5^-		
6454 ± 15			0.49				
6483 ± 5	2^+		0.85			6.52	3^-
6531 ± 10			0.27				
6564 ± 8			0.39				
6634 ± 10	0^+		0.25				
						6.70	2^+
6714 ± 8	4^+		0.65	6.67	2^+		
6744 ± 15							
6772 ± 8	2^+		0.19				
6882 ± 5	1^-		0.25				
6927 ± 15	0^+		2.0	6.84	0^+		
7013 ± 5	3^-		0.95	6.98			
7124 ± 10	4^+		0.31			7.12	
7261 ± 15	(6^+)		0.32				
7289 ± 8			0.61	7.24		7.28	
7338 ± 10			0.13				
7463 ± 8	2^+		0.60	7.42		7.47	2^+
7510 ± 15			0.20				
7611 ± 10	6^+	(T=1)	0.84				

Table 1--Continued.

$(p,t)^{a)}$ E_p=45 MeV				$(p,t)^{b)}$ E_p=40 MeV		$(^3He,n)^{c)}$ $E_{^3He}$=13 MeV	
E_x(keV)	J^π		$\frac{\sigma_{int}}{2\pi}$(μb)	E_x(MeV)	J^π	E_x(MeV)	J^π
7636 ± 15	4^+		0.73	7.58		7.64	
7787 ± 10			0.26				
7817 ± 15	(1^-)		0.16			7.82	
7935 ± 10	2^+		0.60				
8037 ± 15	0^+		0.17			8.05	0^+
8067 ± 8			0.23				
8097 ± 10			0.32				
8122 ± 15	(0^+)		0.13				
8146 ± 10	3^-		0.18				
8184 ± 10			0.27				
8207 ± 8	(3^-)		0.54				
8240 ± 10			0.72				
8327 ± 10	3^-		0.64				
8354 ± 5	2^+	(T=1)	1.6	8.33	(4^+)	8.36	2^+
8401 ± 8	2^+		0.55				
8425 ± 15			0.25				
8461 ± 10							
8511 ± 8	4^+		0.76				
8535 ± 5	4^+	(T=1)	2.7				
8561 ± 5[d)]	0^+	T=2	7.3	8.52	0^+	8.57	0^+
8618 ± 8			0.55				
8661 ± 15	4^+		0.27				
8677 ± 10			0.34				
8727 ± 15							

Table 1--Continued.

$(p,t)^{a)}$ E_p=45 MeV				$(p,t)^{b)}$ E_p=40 MeV		$(^3He,n^{c)})E_{^3He}$=13 MeV	
E_x(keV)	J^π		$\frac{\sigma_{int}}{2\pi}$(μb)	E_x(MeV)	J^π	E_x(MeV)	J^π
8748 ± 10	4^+	(T=1)	1.3				
8770 ± 10	3^-		0.87				
8832 ± 10			0.31				
8872 ± 10							
8900 ± 8	2^+		0.44				
8936 ± 10			0.35				
8962 ± 10[e)]	(6^+)	(T=1)	2.2	8.92			
8985 ± 10							
9044 ± 15	2^+		0.29			9.01	2^+
9059 ± 15	(6^+)		0.46				
						9.13	
9213 ± 8			0.56				
9279 ± 8	4^+	(T=1)	1.3	9.26		9.25	
9311 ± 8							
9338 ± 10			0.76				
9357 ± 15							
9458 ± 10			0.36				
9497 ± 8			0.57			9.47	
						9.77	
10006 ± 5	2^+	T=2	1.4	9.99	2^+		
10049 ± 10			0.56			10.06	2^+
10332 ± 5	0^+		1.5			10.31	0^+

a) Present experiment
b) Ref. 3
c) Ref. 1
d) Doublet of two 0^+ levels separated by ≈ 4 keV
e) Level with probable multiplet structure.

Table 2.--Optical potential and neutron bound state well parameters used in the DWBA calculations.

V	V_o (MeV)	r_o (fm)	a_o (fm)	W (MeV)	W_D (MeV)	r' (fm)	a' (fm)	r_c (fm)	λ^*
protons	47.5	1.25	0.70		13.0	1.25	0.70	1.25	
tritons	173.9	1.15	0.72	20.6		1.50.	0.82	1.40	
bound neutron	V**)	1.25	0.65						2

*) Thomas spin orbit factor.
**) Fitted to a neutron binding energy equal to $\frac{1}{2}(B_{2n}^{g.s}+E_x)$.

Table 3.--Normalization factors used in the DWBA analysis and calculated enhancement factors.

J^π	εD_o^2 exp	(fp) orbitals ε th	(fp) orbitals $D_o^{2***)}$	(sd-fp-$g_{9/2}$) orbitals ε th	(sd-fp-$g_{9/2}$) orbitals $D_o^{2***)}$
0^+	93*)	2.16	43	4.33	21
2^+	44*)	1.49	30	2.26	19
4^+	35*)	1.10	32	1.32	26
6^+	16**)	1.00	16	1.03	16

*) From a comparison of integrated cross section between 6° and 60° to the DWBA cross sections for selected states (see text).

**) The experimental and DWBA cross sections corresponding to the 5.35 MeV state were normalized at 30°.

***) In units of 10^4 MeV^2-fm^3.

Table 4--Comparison of experimental strength with theoretical $f_{7/2}^{-2}$ strength for 0^+ levels.

	experiment			theory	
	E_x(MeV)	a^2	Σa^2	E_x(MeV)	a^2
	0.00	0.510	0.510	0.00	0.558
	4.14	0.018			
	5.36	0.106			
	5.72	0.021			
T=0	6.63	0.007	0.230	7.53	0.181
	6.93	0.068			
	8.04	0.007			
	8.12	0.003			
	10.33	0.050	0.050	10.92	0.011
Total			0.791		0.750
T=2	8.56	0.250		8.06	0.250

Table 5--Same as Table 5 for 2^+ levels

	Experiment			Theory		
	E_x(MeV)	a^2	Σa^2	E_x(MeV)	a^2	Σa^2
	0.85	0.277	0.277	1.05	0.354	0.354
	2.76	0.013				
	4.46	0.023				
	5.83	0.047		5.98	0.031	
	6.48	0.045				
	6.77	0.011	0.279			
T=0	7.46	0.033				
	7.93	0.034				0.063
	8.40	0.032				
	8.90	0.025				
	9.04	0.016				
				9.47	0.003	
				9.94	0.028	
Total			0.556			0.417
	6.03	0.207	} 0.344	5.51	0.343	
	6.04	0.137				
T=1	8.35	0.092	0.092	8.85	0.157	
				10.37	0.000	
Total			0.436			0.500
T=2	10.01	0.083		9.50	0.083	
				11.35	0.000	

Table 6--Same as Table 5 for 4^+ levels

	Experiment			Theory		
	E_x(MeV)	a^2	Σa^2	E_x(MeV)	a^2	Σa^2
	2.39	0.066				
	3.58	0.062	0.128	2.73	0.208	0.208
	5.33	0.049				
	5.48	0.006				
	5.53	0.005				
	5.97	0.014		5.87	0.170	
T=0	6.71	0.037	0.240			
	7.12	0.018				
	7.64	0.044		7.99	0.018	0.209
	8.51	0.049				
	8.66	0.018				
				9.92	0.021	
				10.14	0.000	
Total			0.368			0.417
	6.42	0.263	0.436	6.07	0.424	0.436
	8.54	0.173		7.73	0.012	
T=1	8.75	0.085	0.085	10.16	0.0425	0.045
	9.28	0.090	0.090	11.29	0.019	0.019
Total			0.611			0.500
				10.45	0.000	
T=2				10.69	0.083	

Table 8--Spectroscopic amplitudes and relative enhancement factors δ for the 2h and 2p admixtures in the $^{54}Fe(p,t)^{52}Fe$ reaction.

J	$1d^2_{5/2}$	$2s^2_{1/2}$	$1d^2_{3/2}$	$1f^2_{7/2}$	$2p^2_{3/2}$	$1f^2_{5/2}$	$2p^2_{1/2}$	$1g^2_{9/2}$	$2s_{1/2}1d_{5/2}$	$2s_{1/2}1d_{3/2}$	$1d_{5/2}1d_{3/2}$	$2p_{3/2}1f_{5/2}$	$2p_{3/2}2p_{1/2}$	$2p_{1/2}1f_{5/2}$
								$\frac{S^{1/2}}{(2J+1)^{1/2}}$						
0^-	-0.152	-0.100	-0.225	1	0.141	0.192	0.065	-0.147						
2^+	-0.035		-0.049	1	0.031	0.045		-0.035	-0.042	-0.048	-0.032	0.017	0.034	0.026
4^+	-0.015			1		0.020		-0.018			-0.041	0.022		
6^+				1				-0.010						
								δ						
0^+	0.152	0.132	0.137	1	0.320	0.067	0.082	0.192						
2^+	0.035		0.028	1	0.068	0.016		0.046	0.085	0.069	0.019	0.013	0.094	0.031
4^+	0.015			1		0.007		0.022			0.063		0.044	
6^+				1				0.014						

Table 7--Same as Table 5 for 6^+ levels

	Experiment			Theory		
	E_x (MeV)	a^2	Σa^2	E_x (MeV)	a^2	Σa^2
T=0	4.33	0.088	0.162	4.33	0.207	
	4.87	0.074				
	5.44	0.056	0.098	5.37	0.110	
	6.17	0.042				
	7.26	0.065	0.065	7.82	0.070	
	9.06	0.112	0.112	8.31	0.015	
				11.11	0.016	
Total			0.437			0.417
T=1	5.65	0.287	0.464	5.22	0.287	0.433
	7.61	0.177		7.79	0.146	
	8.96			8.78	0.023	0.023
				11.19	0.043	0.043
Total						0.500
T=2				11.14	0.083	0.083

FIGURE CAPTIONS

1. Spectrum of tritons at 14°.
2. Angular distributions of tritons from $^{54}Fe(p,t)^{52}Fe$ reaction. Lines are drawn to guide the eye.
3. Same as fig. 2.
4. Examples of DWBA fits to experimental angular distributions for even L transfers.
5. The comparison of measured pick-up strength with theoretically predicted $f_{7/2}^{-2}$ strength.
6. Diagrams of the $^{54}Fe(p,t)^{52}Fe$ reaction assuming, (a) the zeroth order process with ^{54}Fe in a pure $(j_p=1f_{7/2})^{-2}_{J_p=0}$ configuration and ^{52}Fe in a pure $(j_p=1f_{7/2})^{-2}_{J_p=0}(j_n=1f_{7/2})^{-2}_{J_n=J}$ configuration, (b) a first order process which includes two-hole admixtures in ^{52}Fe, and (c) a first order process which includes two-particle admixtures in ^{54}Fe. Diagram (d) shows a first order process due to three hole-one particle admixtures with $(j_p=1f_{7/2})^{-2}_{J_p\neq 0}$ in ^{54}Fe.

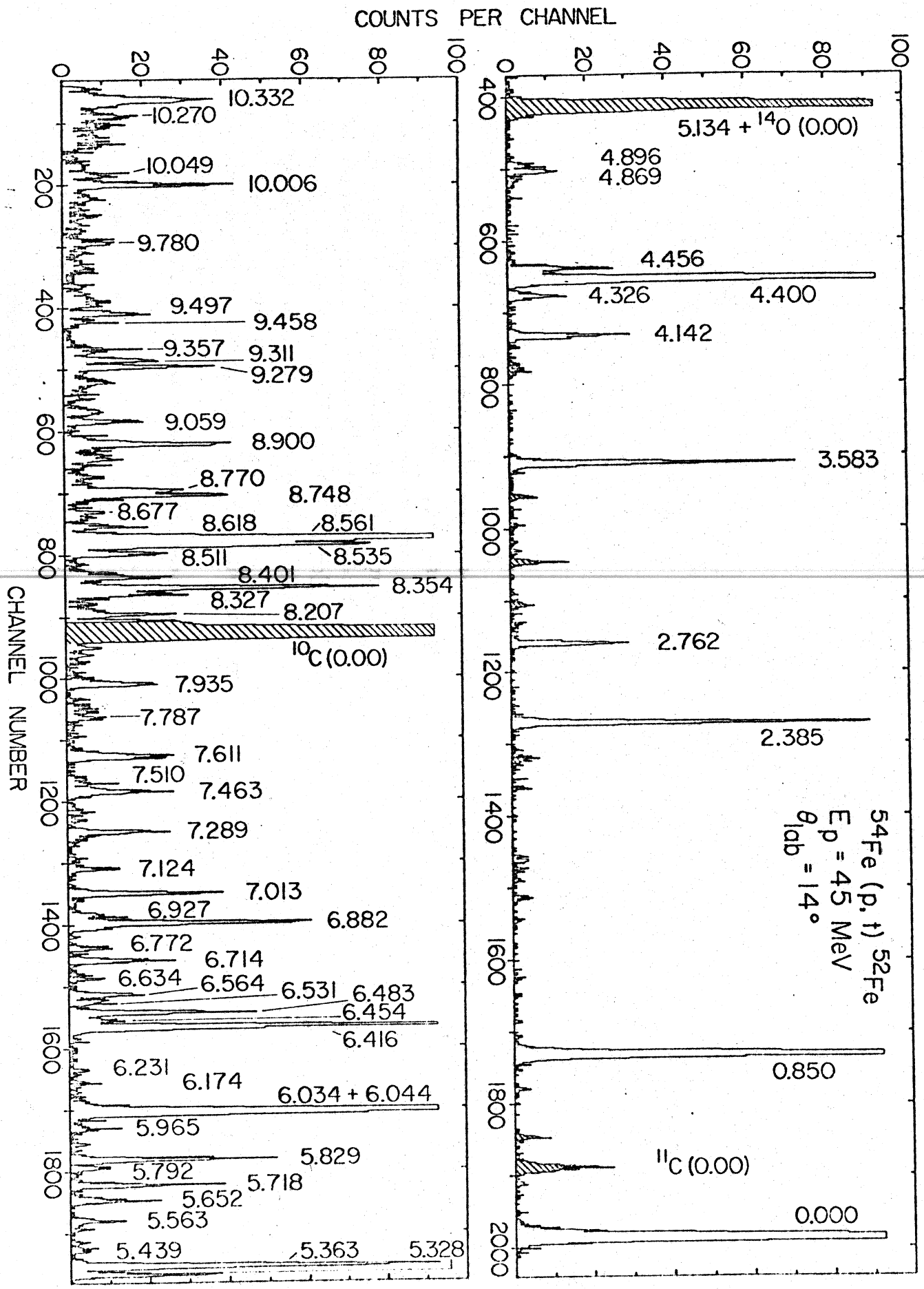
COUNTS PER CHANNEL
CHANNEL NUMBER
54Fe (p, t) 52Fe
Ep = 45 MeV
θlab = 14°
10.332
10.270
10.049
10.006
9.780
9.497
9.458
9.357
9.311
9.279
9.059
8.900
8.770
8.748
8.677
8.618
8.561
8.535
8.511
8.401
8.354
8.327
8.207
10C (0.00)
7.935
7.787
7.611
7.510
7.463
7.289
7.124
7.013
6.927
6.882
6.772
6.714
6.634
6.564
6.531
6.483
6.454
6.416
6.231
6.174
6.034 + 6.044
5.965
5.829
5.792
5.718
5.652
5.563
5.439
5.363
5.328
5.134 + 14O (0.00)
4.896
4.869
4.456
4.326
4.400
4.142
3.583
2.762
2.385
0.850
11C (0.00)
0.000

Figure

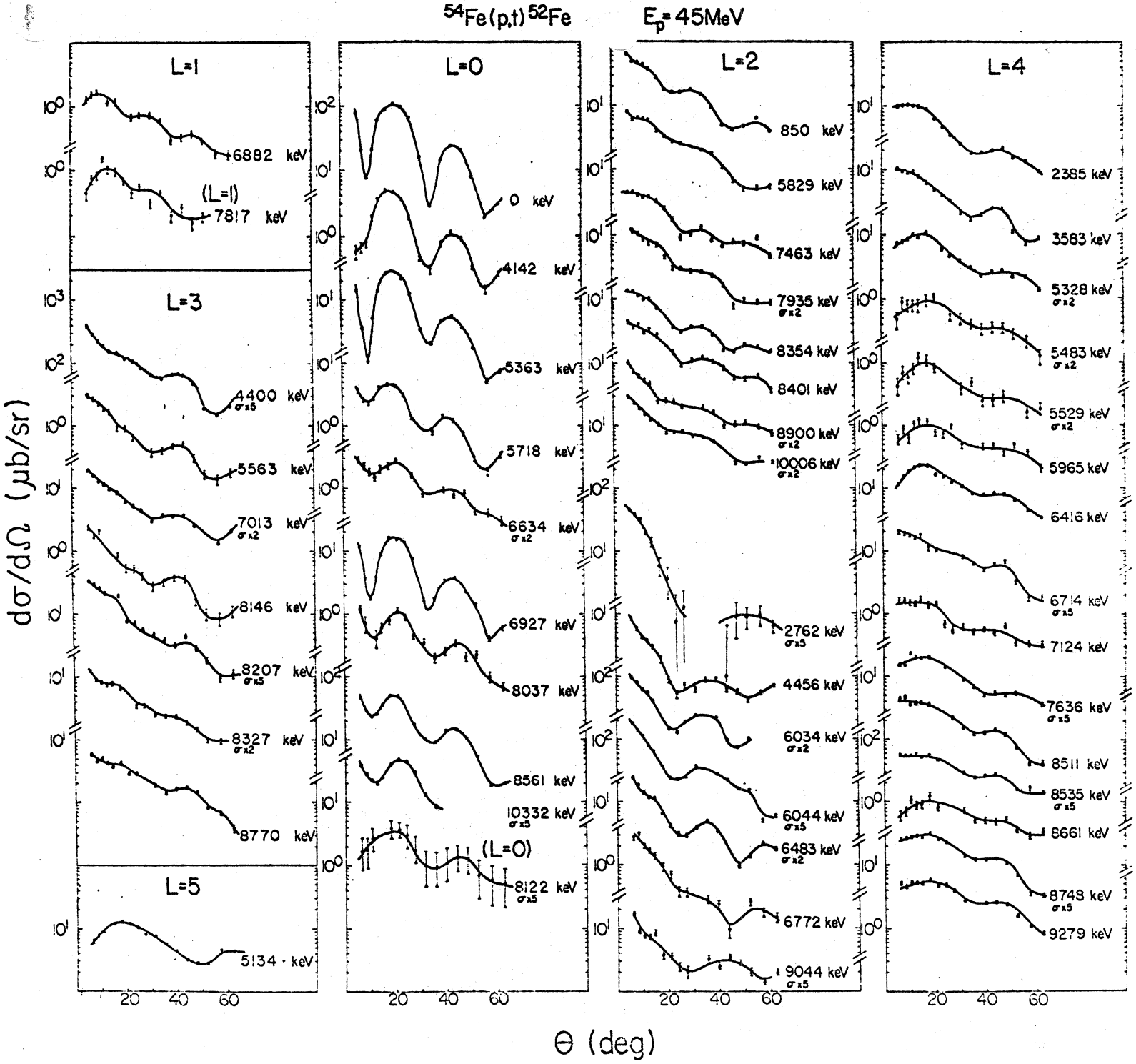
^{54}Fe(p,t)^{52}Fe
E_p= 45MeV
L=1
6882 keV
(L=1)
7817 keV
L=0
0 keV
4142 keV
5363 keV
5718 keV
6634 keV σx2
6927 keV
8037 keV
8561 keV
10332 keV σx5
(L=0)
8122 keV σx5
L=2
850 keV
5829 keV
7463 keV
7935 keV σx2
8354 keV
8401 keV
8900 keV σx2
10006 keV σx2
2762 keV σx5
4456 keV
6034 keV σx2
6044 keV σx5
6483 keV σx2
6772 keV
9044 keV σx5
L=4
2385 keV
3583 keV
5328 keV σx2
5483 keV σx2
5529 keV σx2
5965 keV
6416 keV
6714 keV σx5
7124 keV
7636 keV σx5
8511 keV
8535 keV σx5
8661 keV
8748 keV σx5
9279 keV
L=3
4400 keV σx5
5563 keV
7013 keV σx2
8146 keV
8207 keV σx5
8327 keV σx2
8770 keV
L=5
5134 keV
dσ/dΩ (μb/sr)
Θ (deg)
20
40
60

Figure 2

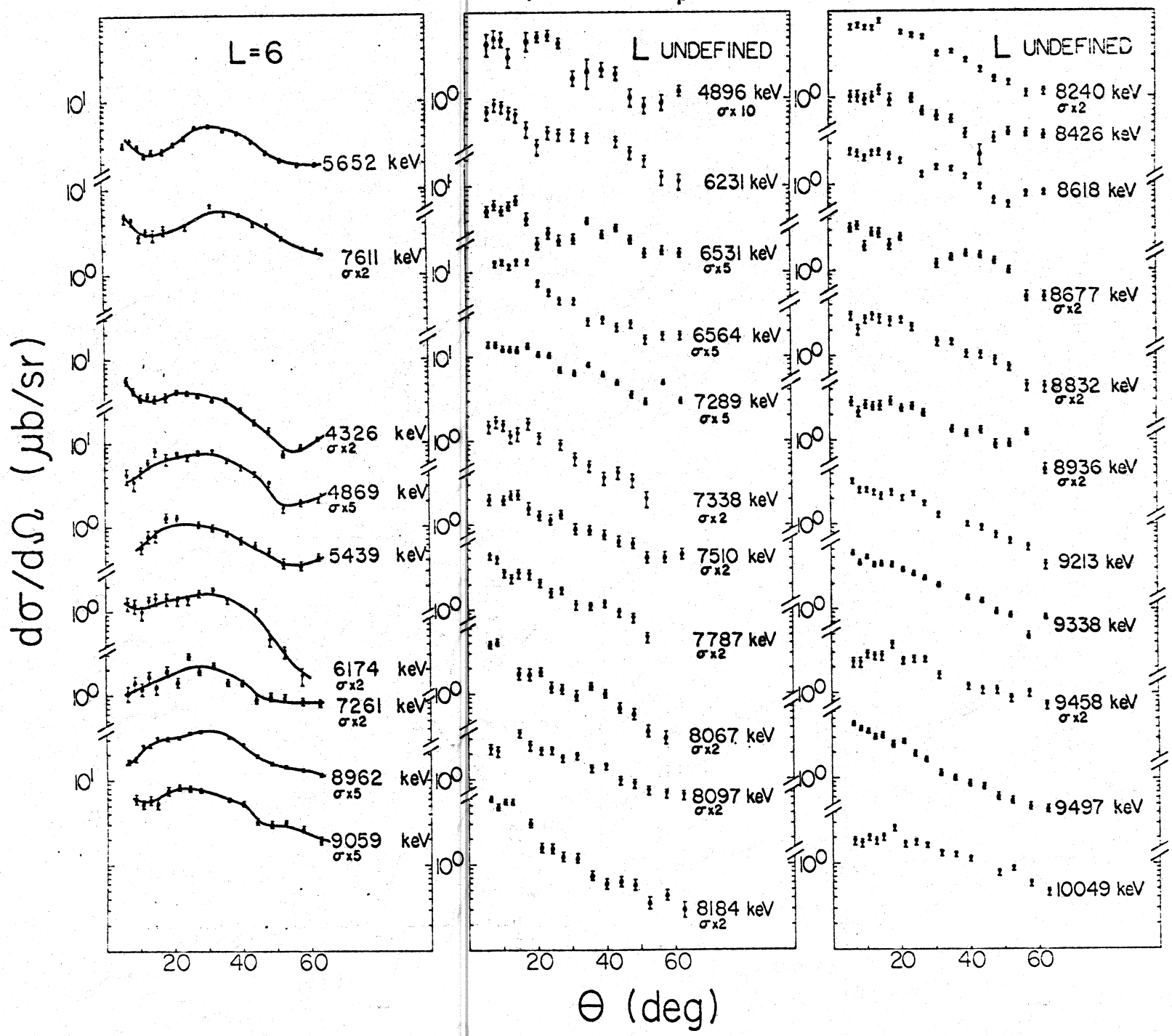
$^{54}Fe(p,t)^{52}Fe$ E_p= 45MeV
L=6
5652 keV
7611 keV σx2
4326 keV σx2
4869 keV σx5
5439 keV
6174 keV σx2
7261 keV σx2
8962 keV σx5
9059 keV σx5
L UNDEFINED
4896 keV σx10
6231 keV
6531 keV σx5
6564 keV σx5
7289 keV σx5
7338 keV σx2
7510 keV σx2
7787 keV σx2
8067 keV σx2
8097 keV σx2
8184 keV σx2
L UNDEFINED
8240 keV σx2
8426 keV
8618 keV
8677 keV σx2
8832 keV σx2
8936 keV σx2
9213 keV
9338 keV
9458 keV σx2
9497 keV
10049 keV
dσ/dΩ (μb/sr)
Θ (deg)
20
40
60
100
10

Figure 3

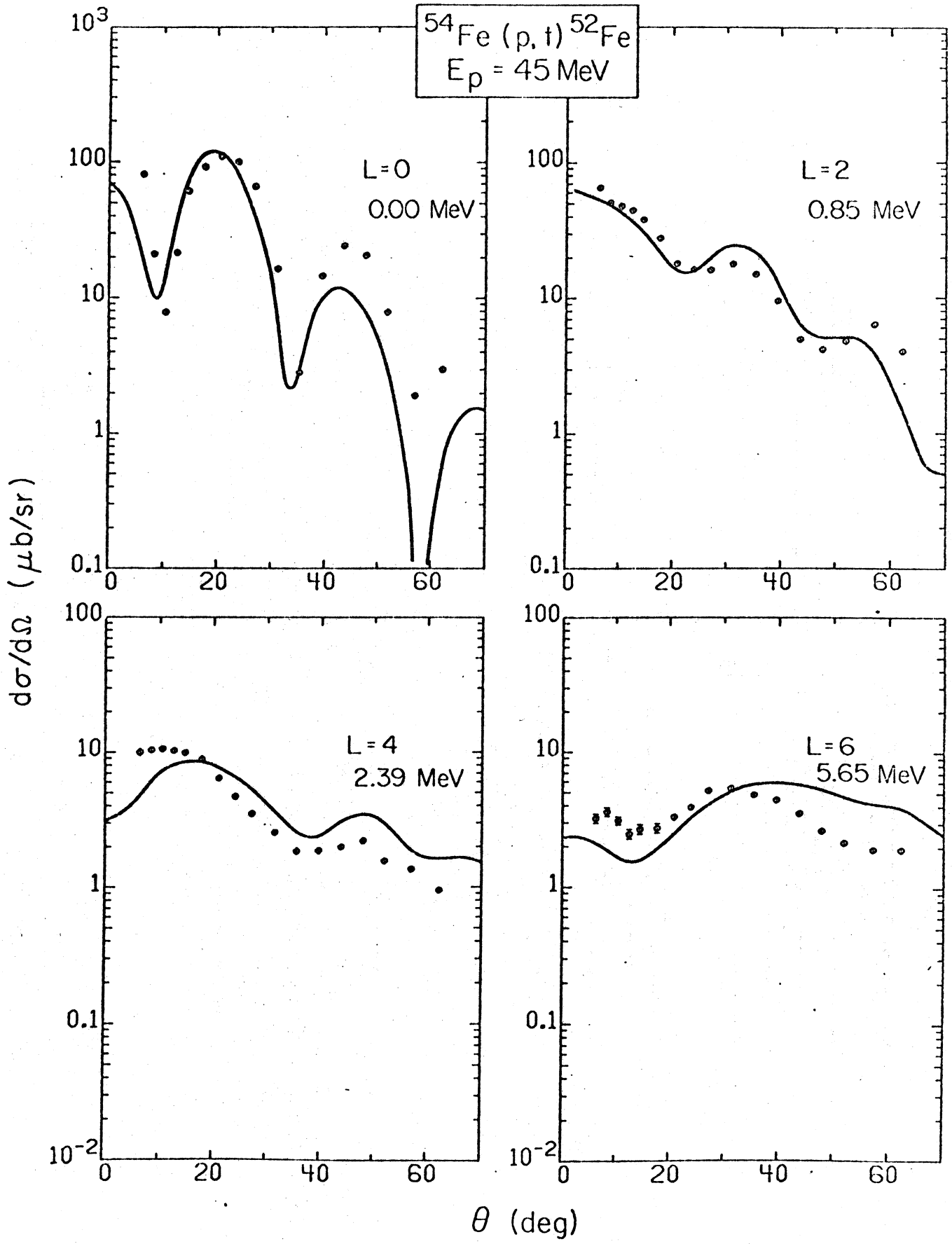
^{54}Fe (p, t) ^{52}Fe
E_p = 45 MeV
L=0
0.00 MeV
L=2
0.85 MeV
L=4
2.39 MeV
L=6
5.65 MeV
dσ/dΩ (μb/sr)
θ (deg)

Figure 4

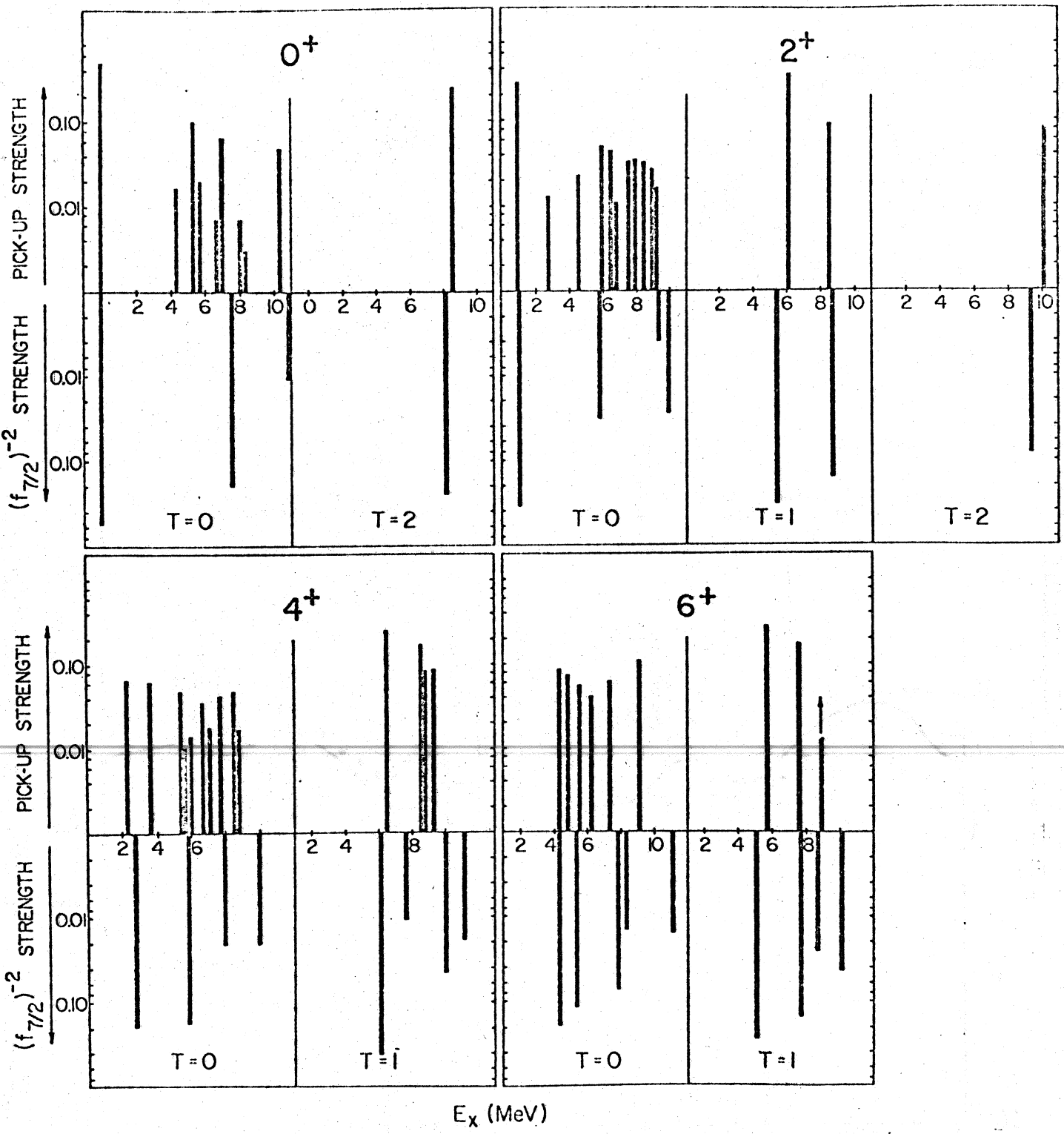
0+
2+
4+
6+
PICK-UP STRENGTH
0.10
0.01
(f7/2)-2 STRENGTH
0.01
0.10
T=0
T=1
T=2
Ex (MeV)

Figure 5

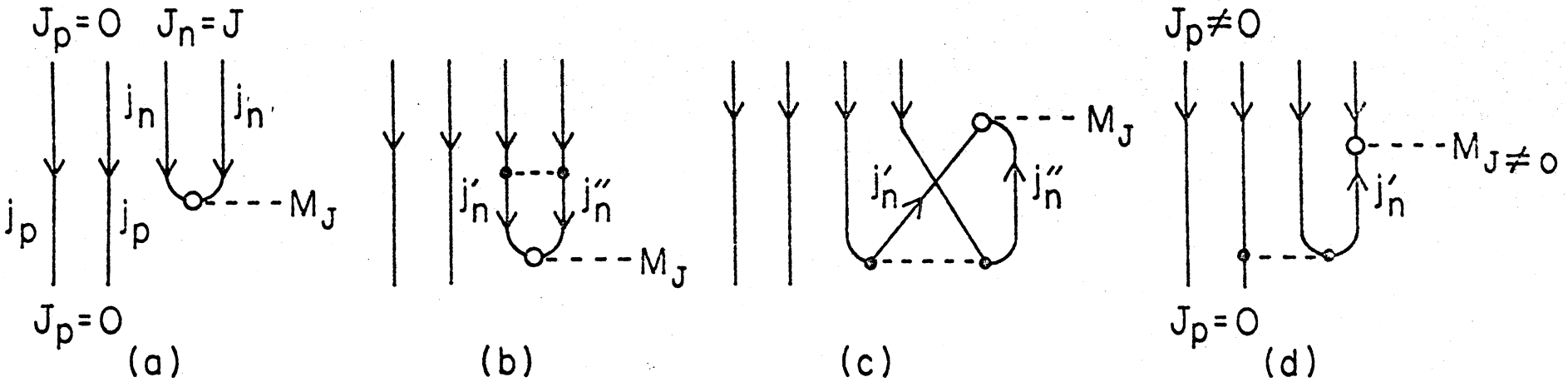
$J_p = 0$
$J_n = J$
j_n
j_n'
j_p
j_p
M_J
$J_p = 0$
(a)
j_n'
j_n''
M_J
(b)
M_J
j_n'
j_n''
(c)
$J_p \neq 0$
$M_J \neq 0$
j_n'
$J_p = 0$
(d)

Figure 6